The High Time Resolution Universe Pulsar Survey – XV. Completion of the intermediate-latitude survey with the discovery and timing of 25 further pulsars

M. Burgay [1]★ B. Stappers,[2] M. Bailes,[3,4] E. D. Barr [5,4] S. Bates,[2] N. D. R. Bhat,[6] S. Burke-Spolaor,[7] A. D. Cameron [8] D. J. Champion,[5] R. P. Eatough,[5] C. M. L. Flynn,[3] A. Jameson,[3,4] S. Johnston [8] M. J. Keith,[2] E. F. Keane [9] M. Kramer,[2,5] L. Levin,[2] C. Ng [10] E. Petroff [11] A. Possenti,[1] W. van Straten [12] C. Tiburzi,[5,13] L. Bondonneau[14] and A. G. Lyne[2]

Affiliations are listed at the end of the paper

ABSTRACT

We report on the latest six pulsars discovered through our standard pipeline in the intermediate-latitude region ($|b| < 15°$) of the Parkes High Time Resolution Universe Survey (HTRU). We also present timing solutions for the new discoveries and for 19 further pulsars for which only discovery parameters were previously published. Highlights of the presented sample include the isolated millisecond pulsar J1826−2415, the long-period binary pulsar J1837−0822 in a mildly eccentric 98-d orbit with a >0.27 M$_\odot$ companion, and the nulling pulsar J1638−4233, detected only 10 per cent of the time. Other interesting objects are PSR J1757−1500, exhibiting sporadic mode changes, and PSR J1635−2616 showing one glitch over 6 yr. The new discoveries bring the total count of HTRU intermediate-latitude pulsars to 113, 25 per cent of which are recycled pulsars. This is the highest ratio of recycled over ordinary pulsars discoveries of all recent pulsar surveys in this region of the sky. Among HTRU recycled pulsars, four are isolated objects. Comparing the characteristics of Galactic fully recycled isolated MSPs with those of eclipsing binaries ('spiders'), from which the former are believed to have formed, we highlight a discrepancy in their spatial distribution. This may reflect a difference in the natal kick, hence, possibly, a different formation path. On the other hand, however, isolated fully recycled MSPs spin periods are, on average, longer than those of spiders, in line with what one would expect, from simple magnetic-dipole spin-down, if the former were indeed evolved from the latter.

Key words: pulsars: individual: J1635−2616, J1638−4233, J1757−1500, J1826−2415, J1837−0822.

1 INTRODUCTION

Pulsars, and in particular the fastest rotating ones, are invaluable tools to explore many aspects of astrophysics and physics: stellar evolution, the interstellar medium and the Galactic magnetic field, plasma physics, relativistic gravity – including gravitational wave emission – and nuclear physics are some of the fields that pulsar studies are contributing to (see e.g. Lyne & Smith 1990; Lorimer & Kramer 2005, and references therein). Finding more pulsars, and

especially millisecond pulsars (MSPs), has led to important steps forward in all of the above topics, and more.

The High Time Resolution Universe Survey (HTRU; Keith et al. 2010) is an experiment searching the majority of the sky visible from the Parkes 64-m radio telescope (NSW, Australia) for radio pulsars and fast transients. The survey, started in 2008 and completed in 2014, is divided into three parts: the first (Ng et al. 2015) covers the lower latitudes ($|b| < 3.5°$) with 70-min pointings, to search for faint pulsars and relativistic binaries in the depths of the Galactic plane; the second covers intermediate latitudes ($|b| < 15°$) and a longitude range from −120° to 30°, with 9-min pointings, with the main aim of finding relatively bright MSPs to be added to pulsar timing array experiments (Bates et al. 2012); the third covers the

★ E-mail: marta.burgay@inaf.it

Table 1. Main parameters of the observing systems adopted for the timing observations. Columns 2–5 report the central frequency, the bandwidth, and the number of frequency channels, while the last column indicates whether the data were coherently or incoherently dedispersed.

Backend	ν_c (MHz)	BW (MHz)	N_{chan}	Dedisp
BPSR	1352	340	871	incoh
DFB3	1369	256	1024	incoh
CASPSR	1352	340	871	coh
APSR	1369	256	512	coh
DFB_{JB}	1532	384	1024	incoh
ROACH	1532	400	1024	coh

rest of the sky accessible at Parkes (with declination $<10°$) with 4-min long pointings, mainly to search for fast transient events, such as Fast Radio Bursts (FRBs; Lorimer et al. 2007; Thornton et al. 2013). The Parkes survey is complemented by a twin experiment (HTRU-North; Barr et al. 2013) carried out at the Effelsberg 100-m radio telescope (Germany).

In this paper we report on the last discoveries made by our standard pipeline (described in Keith et al. 2010) in the intermediate-latitude part of the survey (*HTRU*-med, in the following), and on the timing results of the follow-up campaigns on the new pulsars as well as of 19 other HTRU-med sources for which only discovery parameters have been previously published (Bates et al. 2012).[1] Eight further pulsars, including three MSPs, have been recently discovered in HTRU-med through a novel pipeline and a neural net candidate selection algorithm (Morello et al. 2019).

The paper is structured as follows: in Section 2 we describe the observations and data analysis; in Section 3 we report the results of the timing campaign on 25 HTRU-med pulsars; in Section 4 we present details of the most interesting sources of our sample and in Section 5 we compare the main characteristics of all the 113 HTRU-med pulsars with those of the pulsars found by previous experiments in the same area. Conclusions are drawn in Section 6.

2 OBSERVATIONS AND DATA ANALYSIS

The survey observations and the standard search pipeline used for the discovery of the new pulsars presented in this paper are fully described in Keith et al. (2010). Here we briefly summarize the main points. The 7312 ($\times 13$ beams) 9-min long HTRU-med pointings (whose observing date, beam number and Galactic coordinates are reported in the online supplementary material) were acquired using the Parkes 20-cm Multibeam receiver (Staveley-Smith et al. 1996) and the BPSR digital signal processor (Berkeley Parkes Swinburne Recorder; Keith et al. 2010) over a bandwidth of 400 MHz (340 MHz, after filtering for known Radio Frequency Interferences, RFI) centred at 1382 (1352) MHz. The total bandwidth was split into 1024 frequency channels and the data were 2-bit sampled every 64 µs. This gives $8\times$ better frequency resolution and $2\times$ better time resolution than the previous highest time resolution 20-cm Parkes pulsar surveys (Edwards et al. 2001; Burgay et al. 2006; Jacoby

et al. 2009; Burgay et al. 2013), making HTRU-med particularly sensitive to rapidly spinning and/or high dispersion measure (DM) pulsars.

After time and frequency domain RFI removal, the data were dedispersed using 1196 DM values ranging from 0 to 1000 pc cm^{-3}. Each dedispersed time series was then Fourier transformed and the resulting power spectra were harmonically summed and inspected for significant peaks. Additionally, a single-pulse search in the time domain (whose final results will be reported elsewhere) was performed in parallel. Candidates from all DMs were sorted and the resulting selection was folded for visual (and/or artificial neural network; Bates et al. 2012) inspection. Good candidates were finally reobserved to confirm or reject their astrophysical nature.

Follow-up observations of the new discoveries were initially performed with the same set-up as the survey, using the central beam of the Multibeam receiver only or, for long-period pulsars, folding online with the ATNF digital filterbank DFB3.[2] A grid of five observations, one at the pulsar position and four $0.15°$ to the East, West, North, and South were first performed in order to improve the pulsar position. Observations at the improved position were subsequently obtained at 20 cm either with the Parkes or Jodrell Bank (Manchester, UK) Lovell telescopes, the latter being used for pulsars with declination north of $-35°$. At both telescopes the DFB3 backend was mainly used, except for the MSP follow-up at Jodrell Bank, for which a backend based on ROACH FPGA boards[3] (Bassa et al. 2016), allowing coherent dedispersion, was chosen. A small number of Parkes observations were performed in parallel also with the CASPER Parkes Swinburne Recorder[4] (CASPSR) and the ATNF Parkes Swinburne Recorder[5] (APSR) backends in coherent dedispersion mode, for redundancy. All but the BPSR observations were folded online with sub-integration times ranging from 8 to 32 s. Details of the different observing configurations for timing observations are reported in Table 1.

For the timing analysis, all data archives were preliminarily cleaned of RFI using the interactive PAZI software of the PSRCHIVE package (Hotan, van Straten & Manchester 2004). The archives were then summed in time and frequency to form a single integrated pulse profile per observation. The highest signal-to-noise ratio (S/N) profile was initially adopted as the standard template to obtain the times of arrival (ToAs) from each observation through cross-correlation using PSRCHIVE's PAT application. The ToAs were finally analysed using TEMPO2 (Hobbs, Edwards & Manchester 2006b) to produce a timing model. The planetary ephemeris DE421 (Folkner, Williams & Boggs 2009) and the TT(TAI) time standard (e.g. Lorimer & Kramer 2005) were used. All our timing results are in Barycentric Coordinate Time (TCB). A second iteration of PAT and TEMPO2 was run on the archives after they were updated with the timing model obtained in the previous step, and using, for the cross-correlation, a new noise-free standard template created by using PAAS to fit one or multiple von Mises components to a high-S/N profile obtained summing all the updated archives.

3 NEW DISCOVERIES AND TIMING RESULTS

In this section, after briefly presenting the six new pulsars discovered, we describe the timing results of our follow-up cam-

---

[1]Bates et al. (2012) reports 21 discoveries with no timing solution; for PSR J1825−31 we do not have enough good timing points to give a coherent timing solution yet: the pulsar scintillates and, because of its long period, is severely affected by RFI, hence rarely detected. For PSR J1816−19 (aka J1817−1938) a timing solution has been presented by Knispel et al. (2013), who independently discovered it.

[2]http://www.jb.man.ac.uk/pulsar/observing/DFB.pdf
[3]https://casper.berkeley.edu/wiki/ROACH
[4]http://astronomy.swin.edu.au/pulsar/?topic = caspsr
[5]http://astronomy.swin.edu.au/pulsar/?topic = apsr

Table 2. Discovery parameters of the new pulsars. Columns 2–4 list, for each pulsar, the discovery S/N of the folded profile, the number of the beam in which the pulsar was first detected and the positional offset between its centre and the timing position of the pulsar. The beams are well approximated by a Gaussian with FWHM of ∼14 arcmin (Manchester et al. 2001). The discovery parameters for all HTRU-med pulsars can be found here http://pulsar.oa-cagliari.inaf.it/pulsar/HTRU-med/.

PSR name	S/N	Beam	Δpos (arcmin)
J1518−3952	38.1	01	3.3
J1629−3825	16.3	05	4.7
J1749−5417	11.1	01	6.9
J1824−0132	11.4	03	4.8
J1826−2415	10.3	04	5.9
J1835−0847	18.6	09	1.8

paigns. Details on some specific pulsars of interest are discussed in Section 4. Table 2 lists the discovery parameters of the six new pulsars presented for the first time in this paper. The S/N of the folded pulse profile in the discovery observation, the beam in which the pulsar was detected, and the offset of its centre with respect to the final timing position (see Table 3) are reported.

For Galactic latitudes between ±5° and ±15°, where all new discoveries except PSR J1835−0847 are located, the previous deepest 20-cm search experiment was the Swinburne intermediate-latitude pulsar survey (SWIN$_{MED}$; Edwards et al. 2001), with half the integration time per pointing and 8× worse frequency resolution than HTRU-med. In most cases, the reason why the pulsars in Table 2 were not previously detected, likely lies in their intrinsically low flux densities: usually search candidates with S/N smaller than ∼10 are not visually inspected, or are hard to classify as credible pulsars, hence could have easily been missed. For MSP J1826−2415, moreover, the DM smearing expected from the Swinburne survey is 0.8 ms, a sufficiently large value, compared to the pulsar's spin period, to further reduce the pulse S/N. PSR J1518−3952, on the other hand, has a high discovery S/N and is clearly visible in all our 3-min long timing observations. Folding the closest SWIN$_{MED}$ pointing (whose position is coincident with our discovery pointing) with our timing parameters (see Table 3), indeed, results in a detection with an S/N of 17.5. The vicinity of the pulsar period to 0.5 s (a sub-harmonic of the 50 Hz power line signal) might be the reason why the signal was not considered as a credible candidate.

The only pulsar whose position is not covered by SWIN$_{MED}$ is J1835−0847. The closest observation to its position covered by Parkes surveys is a 35-min long 20-cm observation taken as part of the Parkes Multibeam Pulsar Survey (PMPS; Manchester et al. 2001) 7.8 arcmin away from the pulsar position. Considering the coarser time (4×) and frequency (8×) resolution, the 1-bit sampling and, most importantly, the positional offset, PSR J1835−0847 should have, in PMPS data, an S/N of ∼10, consistent with its non-detection. The positions of PSR J1824−0132 and MSP J1826−2415 are also covered by the outer PMPS pointings. Despite the longer integration time, the positional offsets with respect to the centre of the closest beam and the 3-MHz channels, make the expected S/N too low for a firm detection.

Table 3. Main timing parameters for 25 HTRU-med pulsars. Columns 1 and 2 report the pulsar name and the provisional name used in Bates et al. (2012). Columns 3–8 report J2000 right ascension and declination, spin period and spin period first derivative, the epoch at which the period is referred, and the dispersion measure. The last three columns report the data span of the timing observations, the rms of the timing residuals, and the number of ToAs. Numbers in parentheses are the 2σ errors on the last quoted digit(s).

PSR name	Alias	RA J (h:m:s)	Dec. J (d:m:s)	P (s)	Ṗ (10⁻¹⁵)	EPOCH (MJD)	DM (pc cm⁻³)	Data span (MJD)	rms (ms)	N(ToA)
J0836−4233	J0835−42	08:36:05.85(3)	−42:33:24.9(3)	0.73843560627(4)	1.320(4)	56290	180	55954–56626	0.64	26
J1105−4353	J1105−43	11:05:24.84(11)	−43:53:05(3)	0.35111186198(7)	2.50(4)	55976	45	55804–56147	0.94	14
J1132−4700	J1132−46	11:32:14.52(3)	−47:00:36.5(3)	0.325633290107(6)	0.7768(7)	56122	123	55756–56488	0.63	36
J1518−3952	–	15:18:56.968(18)	−39:52:30.3(7)	0.499195890475(15)	0.237(8)	56442	101	56256–56627	0.27	25
J1530−6343	J1530−63	15:30:47.608(20)	−63:43:13.6(3)	0.910319586358(11)	0.825(7)	56093	206	55906–56279	0.19	28
J1551−6214	J1552−62	15:51:36.788(8)	−62:14:23.37(9)	0.1988386042970(8)	0.0228(5)	56108	122	55905–56310	0.08	24
J1614−3846	J1614−38	16:14:42.52(8)	−38:46:35(6)	0.46410631422(9)	0.92(4)	55876	111	55698–56054	1.33	17
J1629−3825	–	16:29:14.618(11)	−38:25:29.3(5)	0.526364586499(9)	0.4438(14)	56376	127	56125–56626	0.37	34
J1636−2614^a	J1635−26	16:36:11.506(17)	−26:14:47.0(13)	0.510453755610(8)	4.0580(11)	57018	94	55910–58127	0.29	95
J1638−4233	J1638−42	16:38:24.71(6)	−42:33:55(3)	0.51092936864(3)	10.088(3)	56253	406	55834–56672	0.86	9
J1704−5236	J1705−52	17:04:40.569(15)	−52:36:57.4(5)	0.230708491737(3)	0.05.2(3)	56108	170	55905–56311	0.30	24
J1719−2330^b	J1719−23	17:19:36.1(4)	−23:30:14(72)	0.453992694395(19)	2.1861(4)	56614	101	55690–57848	3.15	75
J1749−5417	–	17:49:47.06(3)	−54:17:30.7(3)	0.307576751860(6)	0.1496(7)	56388	69	56066–56709	0.44	23
J1757−1500^b	J1757−15	17:57:12.752(17)	−15:00:28.5(17)	0.179354019096(13)	1.5039(4)	57038	150	55955–58121	1.82	128
J1802−0523	J1802−05	18:02:12.14(8)	−05:23:29(4)	1.68057296916(9)	2.649(3)	56908	121	55696–58119	8.95	104
J1818−0151	J1818−01	18:18:25.77(3)	−01:51:54.0(11)	0.837534946983(11)	9.1061(5)	57015	209	55909–58120	2.39	78
J1824−0132	–	18:24:55.575(9)	−01:32:24.0(4)	0.223728519703(4)	0.02.82(3)	57658	79	57182–58133	0.67	43
J1826−2415	–	18:26:36.0260(9)	−24:15:54.5(3)	0.0046957571305605(7)	0.00001736(3)	57054	81	55957–58152	0.03	97
J1835−0847	–	18:35:45.72(5)	−08:47:20(3)	0.84649413462(6)	0.485(4)	57653	850	57183–58123	2.83	45
J1837−0822	J1837−08	18:37:39.654(10)	−08:22:12.4(7)	1.099195959243(8)	0.1209(3)	57036	506	55955–58117	1.10	122
J1840−0445^b	J1840−04	18:40:45.5(3)	−04:45:08(13)	0.42231632097(13)	11.280(3)	57053	379	55955–58151	28.32	94
J1900−0933	J1900−09	19:00:31.19(3)	−09:33:48.1(15)	1.423889144409(19)	0.2263(9)	56979	189	55840–58118	2.43	103
J1902−1036^b	J1902−10	19:02:42.399(10)	−10:36:13.0(7)	0.786813538431(8)	7.53681(19)	56916	91	55699–58124	0.99	95
J1904−1629	J1904−16	19:04:51.37(3)	−16:29:19(3)	1.541412044233(20)	3.1900(8)	57039	145	55956–58119	1.45	58
J1920−0950	J1920−09	19:20:55.93(3)	−09:50:01.0(18)	1.037824001161(19)	0.3928(7)	57037	93	55955–58119	2.66	79

Notes. ^{a}For this pulsar we report the pre-glitch parameters and rms, but the total number of ToAs acquired over the entire data span.

^{b}For these pulsars also a spin frequency second derivative was fitted (see Section 4.5.2).

Table 4. Derived parameters and other measured parameters for 25 HTRU-med pulsars. Column 2 and 3 report the Galactic longitude and latitude; columns 4 and 5 the DM-derived distances obtained using the NE2001 (Cordes & Lazio 2002) and YMW16 (Yao, Manchester & Wang 2017) models for the distribution of free electrons in the Galaxy, respectively. We note that the values obtained by the two models are, in some cases, significantly different, with the YMW17 model often giving very large distances. Columns 6–8 list the dipolar surface magnetic field, the spin-down energy, and the characteristic age of the pulsars. The last three columns report the pulse width at 50 and 10 per cent of the pulse height, and the pulsar mean flux density at 1.4 GHz.

PSR name	l (°)	b (°)	D_{DM}^{ne2001} (kpc)	D_{DM}^{ymw16} (kpc)	B_{surf} (10^{11} G)	$\dot{E}$ (10^{32} erg s^{-1})	τ_c (10^6 yr)	W50 (ms)	W10 (ms)	S_{1400} (mJy)
J0836−4233	261.537	−1.107	0.5	3.6	9.9	1.3	8.9	14.21(1)	25.91(1)	0.129(3)
J1105−4353	283.486	14.947	1.6	0.1	9.5	22.8	2.2	13.107(5)	23.923(5)	0.189(6)
J1132−4700	289.177	13.736	5.2	2.7	5.1	8.9	6.6	17.6(5)	29.0(3)	0.490(5)
J1518−3952	331.368	14.715	3.2	11.4	3.5	0.8	33.4	7.6(1)	55.2(6)	0.90(1)
J1530−6343	319.506	−6.101	5.0	11.5	8.8	0.4	17.5	11(5)	32.6(3)	0.37(9)
J1551−6214	322.300	−6.350	2.7	3.9	0.7	1.1	138.0	2.8(1)	6.46(6)	0.312(5)
J1614−3846	340.628	8.788	2.7	5.7	6.6	3.7	7.9	24.471(6)	44.726(6)	0.182(6)
J1629−3825	342.889	7.006	2.9	5.6	4.9	1.2	18.8	7.0(3)	14.8(3)	0.383(4)
J1636−2614	353.120	14.036	2.9	8.3	14.6	12.0	1.9	7.273(4)	13.271(7)	0.19(5)
J1638−4233	341.007	2.924	7.6	22.2	23.0	29.9	0.8	18(1)	44(3)	0.35(1)
J1704−5236	336.051	−6.869	4.0	9.6	1.1	1.7	70.1	15.3(3)	24.1(5)	0.605(9)
J1719−2330	1.402	7.846	2.4	4.3	10.1	9.2	3.3	8.9(6)	18.0(4)	0.16(6)
J1749−5417	338.275	−13.427	1.8	3.3	2.2	2.0	32.6	12.133(3)	22.153(4)	0.321(9)
J1757−1500	13.367	4.785	3.3	4.3	5.3	103.0	1.9	2.1(7)	4.78(5)	0.09(2)
J1802−0523	22.425	8.398	3.4	4.1	21.4	0.2	10.1	64.4(5)	146(3)	0.15(7)
J1818−0151	27.482	6.479	6.2	19.3	27.9	6.1	1.5	15(1)	35.1(9)	0.09(2)
J1824−0132	28.525	5.188	2.3	3.1	0.8	0.9	126.0	7.4(2)	22.4(6)	0.12(5)
J1826−2415	8.553	−5.718	2.3	2.8	0.003	66.2	4290	0.361(1)^a	1.9(9)^a	0.28(9)
J1835−0847	23.331	−0.548	9.4	6.2	6.5	0.3	27.6	46(1)	108(5)	0.4(1)
J1837−0822	23.918	−0.772	6.7	5.2	3.7	0.03	144.0	37(3)	53.7(3)	0.2(2)
J1840−0445	27.486	0.203	6.0	4.6	22.1	59.1	0.6	22.4(7)	53(2)	0.37(8)
J1900−0933	25.413	−6.346	5.2	13.7	5.7	0.03	99.7	51(19)	250(2)	0.4(2)
J1902−1036	24.716	−7.291	2.6	3.8	24.6	6.1	1.7	11.80(1)	21.528(7)	0.13(7)
J1904−1629	19.590	−10.332	4.6	25.0	22.4	0.3	7.7	12.4(9)	30.8(4)	0.17(7)
J1920−0950	27.417	−10.977	3.0	6.2	6.5	0.1	41.9	39.2(6)	60(1)	0.20(8)

Note. ^{a}The values reported in the table are for the main peak only. The 50 and 10 per cent widths of the secondary peak are 0.5(2) and 1.8(8) ms, respectively.

Folding the archival data[6] closest to our new pulsar positions with the ephemeris we obtained in our timing campaign (see Table 3), resulted indeed, besides the aforementioned case of J1518−3952, in only faint detections of J1835−0847 (S/N = 10.1 after RFI removal), J1826−2415 (S/N = 9.5), and J1824−0132 (S/N = 10.3) in PMPS data, and of J1629−3825 in SWIN$_{MED}$ (S/N = 10.9), and the Parkes 70-cm all-sky survey (S/N = 12.2; Manchester et al. 1996). These low-S/N detections from archival data are not included in our timing solutions, due to unknown instrumental offsets.

Timing observation of the pulsars presented here spanned, at Parkes, on average 400 d for each pulsar, except for the nulling PSR J1638−4233 (Section 4.3), observed for twice as long because of the paucity of detections. Lovell telescope observations, on the other hand, continued for longer, and in most cases are still ongoing as of 2018 August.

In Table 3 we list the main timing parameters for the latest 25 pulsars (6 new and 19 whose discovery was reported in Bates et al. 2012) discovered in HTRU-med through our standard FFT-based, non-accelerated pipeline, while in Table 4 we list the parameters derived from the timing analysis, along with the widths of the pulse profiles, and the pulsars mean flux densities at 20 cm. For the pulsar timed at Jodrell Bank (with declinations above −35°), the flux densities are estimated averaging the values obtained through the radiometer equation (e.g. Manchester et al. 2001) for each single observation, and the errors are their standard deviation. Given the

fact that timing observations with the Lovell telescope were done at low elevation, gain loss and spill-over effects have also been taken into account. Parkes' values, instead, are obtained through calibrated data using PSRCHIVE's PAC.

The 25 pulsars in our sample are shown as large stars in the period–period derivative diagram of Fig. 1, together with the other previously published HTRU-med pulsars (small black stars), and the rest of the known Galactic field radio pulsar population (grey dots) as derived from version 1.58 of the ATNF Pulsar Catalogue[7] (Manchester et al. 2005).

Fig. 2 shows the integrated pulse profiles for our sample of pulsars, obtained by summing, for each source, the entire 20-cm data set used for timing (see Table 3). The total summed integration time contributing to each profile is shown in the top left corner of the plot. Observations are uncalibrated, hence the *y*-axis is in arbitrary units. For the pulsars observed at Parkes, the data were folded over 512 time bins, while for those observed at Jodrell Bank 1024 bins were used. In both cases the profile bins were reduced to 256 for plotting purposes only. DM smearing is smaller than the shown time bin in all cases.

4 HIGHLIGHTS

In the following sub-sections we discuss in more detail the most interesting features of some of the pulsars presented in this paper.

[6]Obtained through the Parkes Data Access Portal https://data.csiro.au/dap/public/atnf/pulsarSearch.zul
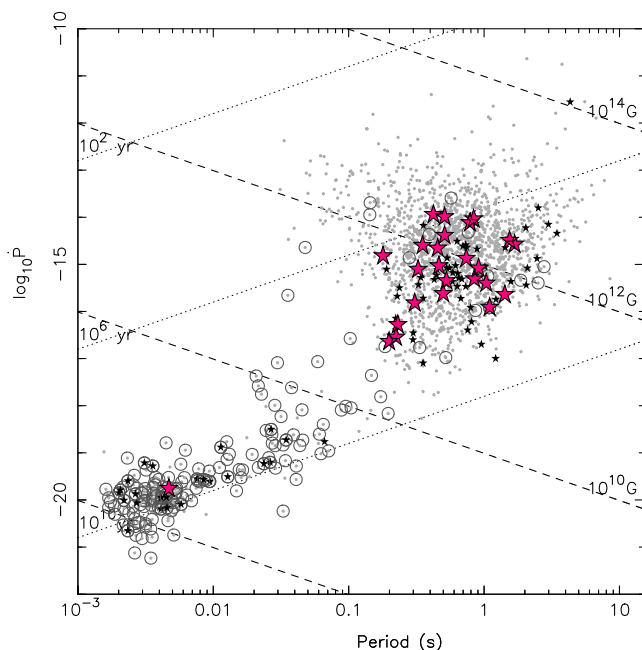
[7]http://www.atnf.csiro.au/people/pulsar/psrcat/

Figure 1. Period–period derivative diagram. Large pink stars are the 25 pulsars presented in this work. Small black stars are the other HTRU-med pulsars discovered with our standard pipeline. Grey dots are previously known Galactic field radio pulsars. Binary pulsars are surrounded by a grey circle. Dashed and dotted lines are equal magnetic field and equal characteristic age lines, respectively. Data were obtained from the ATNF Pulsar Catalogue (Manchester et al. 2005) v. 1.58.

4.1 PSR J1837−0822: a long-period pulsar in a 98-d orbit

PSR J1837−0822 is a 1.1-s pulsar in a 98-d, mildly eccentric orbit ($e = 0.024$; see Table 5) around a low-mass companion star. This pulsar is one of only 21 known long-period (P > 0.1 s) pulsars in a binary system in the Galactic field.

The minimum mass of the companion, derived from the mass function assuming a 1.35 $M_\odot$ neutron star (NS), is 0.27 $M_\odot$ for an edge-on orbit. The median companion mass, calculated for an inclination angle of $60°$, would be 0.32 $M_\odot$, and could be as high as 0.41 $M_\odot$ for a pulsar mass of 2 $M_\odot$ (the highest NS mass precisely measured; Antoniadis et al. 2013). A 90 per cent confidence upper limit on the companion mass can be obtained using an orbital inclination angle of $26°$: depending on the NS mass (1.35 or 2 $M_\odot$), the maximum mass for PSR J1837−0822's companion ranges from 0.73 to 0.9 $M_\odot$.

The intermediate eccentricity of this system, together with its long spin and orbital periods and its relatively small companion mass (see Table 5), likely makes it the third example of a weakly (if at all) recycled long-period pulsar (Tauris, Langer & Kramer 2012), together with J1932+1500 (Lyne et al. 2017a) and J1822−0848 (Lorimer et al. 2006). Similarly to the other two, the eccentricity of PSR J1837−0822's orbit is too small for the pulsar to be a non-recycled object relatively recently born in a binary system like e.g. PSR J2032+4127 (Lyne et al. 2015) or PSR J1740−3052 (Lorimer et al. 2006), in eccentric orbits around massive main-sequence stars, or like PSR J1141−6545 (Tauris & Sennels 2000), an NS born after its white dwarf (WD) companion. On the other hand, the eccentricity is too high for the system to be similar to mildly recycled pulsars, having typically lower spin periods ($\lesssim$0.1 s) and magnetic fields ($\lesssim$10^{10} G). As further evidence of its peculiarity, PSR J1837−0822 does not follow the orbital period–eccentricity relation of Phinney

(1992) for Helium WD (He-WD) companions and falls close to the other two members of this new small family, in the P_b–e plot (see Fig. 3).

The position of these three pulsars in the plot, together with their long spin periods (distinguishing them, e.g. from the close-by CO-WD systems, with almost two orders of magnitude smaller rotational periods), puts them in a peculiar category of binary pulsar whose companions have likely evolved into He-WDs via mass transfer, but in which accretion on to the NS has not taken place in an effective way, or at all (Tauris et al. 2012).

4.2 PSR J1826−2415 and the origin of isolated MSPs

Isolated fully recycled MSPs (defined here as pulsars with spin periods smaller than 10 ms and magnetic fields smaller than 10^9 G) are relatively rare in the Galactic field. The ATNF pulsar catalogue lists only 32 such objects. Another 23 MSPs with no orbital period measured are listed in the catalogue; these however, have no fully coherent timing solutions yet (only the discovery parameters with a small number of significant digits are listed), and/or they do not have a measured spin period derivative yet. Because of this, we cannot be certain that they do not have a companion star, at the moment, and in the following we define them as isolated candidates. PSR J1826−2415, a 4.7-ms isolated pulsar, adds to this small and interesting family of objects whose origin is still under debate.

In the standard scenario, isolated MSPs are the end product of binary systems where the pulsars have completely ablated their companion stars (e.g. Alpar et al. 1982; van den Heuvel & van Paradijs 1988; Bhattacharya & van den Heuvel 1991). In this framework, the so-called Black Widows and Redbacks (hereafter 'spiders'), binary systems where the radio signal from the MSP is eclipsed for a significant fraction of the orbit by matter stripped from their companions (see e.g. Roberts 2013), would be the progenitors of isolated MSPs. Whether or not the time-scale for complete ablation of the companion star is short enough, however, is still debated (e.g. Kulkarni & Narayan 1988; Ruderman, Shaham & Tavani 1989; Stappers et al. 1996; Chen et al. 2013).

Because of pulsar spin-down, if this model is correct, one would expect isolated MSP to have longer spin periods P than the spiders from which they derive. P distributions of Redbacks and Black Widows (both counted separately and all together) have indeed mean and median values ∼2 ms smaller than those of isolated MSPs (see Table 6), supporting the standard scenario. The numbers in 6 are for Galactic field objects only, since the evolutionary history of the systems in Globular Clusters could be dramatically different (e.g. Verbunt et al. 1987).

An observational parameter that, on the other hand, we would expect to be similar in isolated MSPs and spiders, if in fact they had a common origin, is their distance from the Galactic plane Z, a parameter linked to the natal kick velocity of pulsars, hence to their formation path. Looking at the average values of Z for the various classes of Galactic field MSPs, instead, we see that spiders are, on average, further from the plane (with a mean vertical distance $Z_{mean} = 0.8$ kpc), while isolated MSPs appear on average lower ($Z_{mean} = 0.3$ kpc) and more similarly distributed to non-eclipsing binaries ($Z_{mean} = 0.4$ kpc[8]). This seems to argue against a common origin between spider MSPs and the bulk of the isolated

---

[8]The numbers above are calculated in PSRcat using the distance from the Yao et al. (2017) electron density model. Compatible results, with spiders having Z_{mean} twice as big as that for isolated and non-eclipsing binaries, are obtained using the Cordes & Lazio (2002) model.
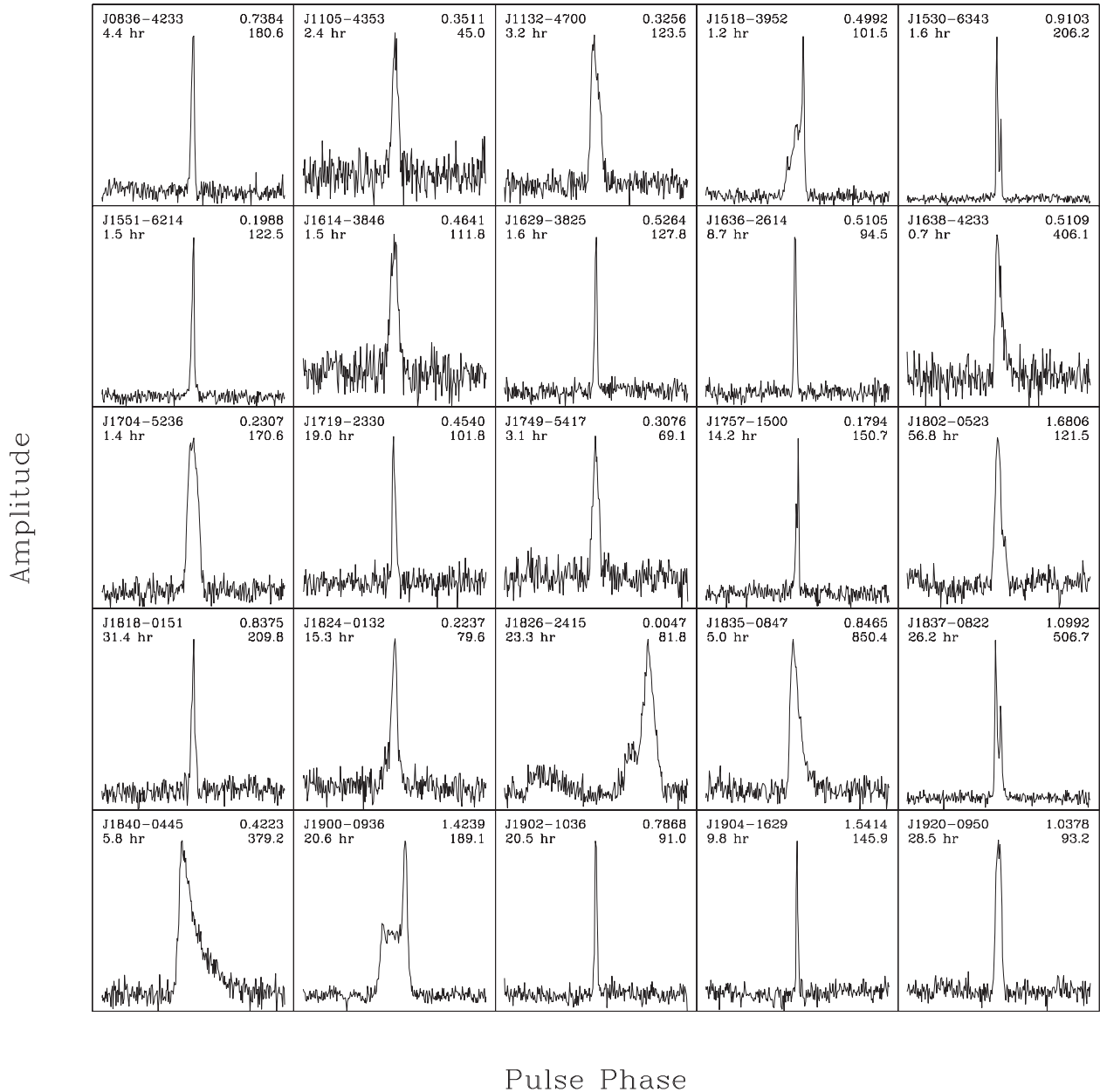
Figure 2. Integrated pulse profiles for the 25 pulsars presented here. For each pulsar, in the top left corner we report the source name and the integration time contributing to the pulse profile, and in the top right corner the spin period in seconds and the dispersion measure in $\mathrm{pc\,cm^{-3}}$. The entire pulse period is shown.

ones (although we must note that, deriving from the quite uncertain DM-inferred distances, Z values may have large errors). Alternative scenarios, such as accretion-induced collapse of a WD (Bailyn & Grindlay 1990), or WD mergers (Michel 1982), appear to be more in line with a low velocity at birth (hence possibly a small distance from the Galactic plane) for isolated MSPs; a high velocity and a high altitude are expected for tightly bound systems (Tauris & Bailes 1996) such as Redbacks and Black Widows, and such as isolated MSPs would need to have been, if they had to be able to efficiently ablate their companions.

4.3 The nulling pulsar J1638−4233

PSR J1638−4233 was observed at Parkes 52 times, for a total of 4.9 h over a period of 3 yr. Single observations typically lasted 5 min.

In total, J1638−4233 was seen (S/N > 7) on only nine occasions. Fig. 4 shows the number and time of detections for this pulsar.

Even when the pulsar is visible, its pulses appear to switch off (or null; Backer 1970b) for times extending from a single sub-integration (20 or 30 s, depending on the time resolution of each observation) to a few minutes: the longest gap between two ON phases in a single observation is 2 min, while the longest observation in which the pulsar is always off is 10 min. To better estimate the duration of the nulling phases of the observations in which the pulsar is seen, we cross-correlated the pulsar's standard profile with all the sub-integrations in the data files, and counted as OFF all the sub-integrations for which the time of arrival was more than 0.1 pulsar rotations off with respect to zero phase predicted on the basis of the timing solution presented in Section 3. About one third of the sub-integrations appear to be off. Considering this and the

Table 5. Orbital parameters for the binary long-period pulsar J1837−0822. The BT binary model (Blandford & Teukolsky 1976) was adopted. Row 1–6 list the orbital period, the projected semimajor axis, the epoch and the longitude of the periastron, the eccentricity and the mass function. The minimum ($M2_{min}$), median ($M2_{med}$), and maximum ($M2_{max}$) companion masses (see text) were obtained assuming a 1.35 $M_{\odot}$ NS mass. 2σ errors on the last quoted digit(s) are reported in parentheses.

PSR J1837−0822	
P_b (d)	98.36371(3)
$a1$ (lt-s)	40.8780(4)
T0 (MJD)	55978.1170(10)
ω (°)	21.94(4)
e	0.024319(15)
f_m ($M_{\odot}$)	0.0075802(2)
$M2_{min}$ ($M_{\odot}$)	0.27
$M2_{med}$ ($M_{\odot}$)	0.32
$M2_{max}$ ($M_{\odot}$)	0.73
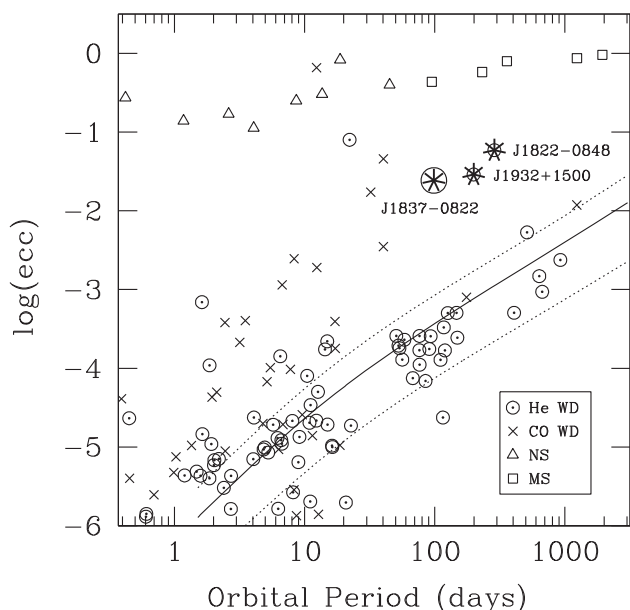
Figure 3. Orbital eccentricity versus orbital period of binary pulsars in the Galactic field. Circled dots are pulsars with He-WD companions, crosses have carbon–oxygen companions (CO-WD), while triangles and squares denote pulsars with NS and main sequence (MS) companions, respectively (from the ATNF pulsar catalogue; Manchester et al. 2005). According to the model of Phinney & Kulkarni (1994), 95 per cent of recycled pulsars with low-mass He-WD companions should fall within the dotted lines. The large asterisks are the three long period binary pulsars J1837−0822, J1932+1500, and J1822−0848.

Table 6. Mean and median spin periods (columns 3 and 4) for isolated MSPs (bona fide ones, first line, and including candidates, second line), Redbacks, Black Widows, and spiders all together. Column 2 lists the number of pulsars in each category.

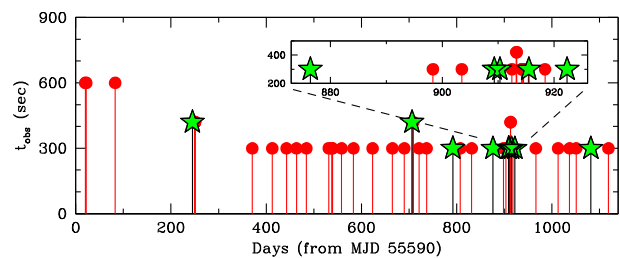| Type	#PSRs	P_{mean} (ms)	P_{med} (ms)
Isolated	32	4.47	4.72
Isolated + cands	55	4.59	4.39
Redbacks	12	3.15	2.75
Black Widows	22	2.58	2.32
Spiders	34	2.79	2.48

Figure 4. Detections (green stars) and non-detections (red circles) of PSR J1638−4233 plotted in a time (days from MJD 55590) versus observation length plot. The pulsar was seen on only nine occasions. The inset is a blow-up the MJD range 56463-56516, when more than half of the detections were made.

non-detections, the total nulling fraction is about 90 per cent, among the highest known (see e.g. Wang, Manchester & Johnston 2007; Gajjar 2017), with the pulsar ON for only about 33 min of the 4.9 observed hours.

Given that more than half of the detections occurred in a short time span (5 over 45 d, 4 of which over 13 d), it could also be that PSR J1638−4233 is both a nulling and an intermittent pulsar (Kramer et al. 2006; Camilo et al. 2012; Lorimer et al. 2012; Surnis et al. 2013), switching off for long periods, and being a nuller with a null fraction of about 50 per cent, in its active state. In its longer term behaviour it could be similar to PSRs J1910+0517 and J1929+1357 (Lyne et al. 2017b) which show extreme bimodal long-term intermittency. The latter shows changes in the spin-down rate which is correlated with a change in the fraction of time it was on (Lyne et al. 2017b). Unfortunately the detections are too sparse to check if there are correlated spin-down changes in PSR J1638−4233, but increased monitoring, perhaps by MeerKAT (Jonas 2009), the recently opened South African precursor of the Square Kilometre Array, could reveal if it is indeed a member of the intermittent class.

4.4 Mode changes in PSR J1757−1500

Sometimes linked to nulling, mode changing (e.g. Wang et al. 2007; Lyne et al. 2010) is a phenomenon, observed now in a few tens of pulsars, where the integrated pulse profile switches between two or more quasi-stable states (in the case of nulling, in the second state the pulse is off).

When timing PSR J1757−1500, a faint pulsar with a 0.18 s spin period, we noticed that a small number of timing points appeared offset with respect to the rest (see Fig. 5). Fitting a constant phase jump (from MJDs 56838 to 57238, around the epoch where most of the offset points are, to avoid the effects of timing noise; see 4.5.2), we obtain a value of 0.00179(6) s, compatible with the separation of ∼ 0.01 in pulse phase between the two components of the pulse profile.

Upon closer inspection, indeed, the (5-min long) observations to which the phase jump had to be applied appear, when the noise in the profile is low enough to make a distinction, to be single peaked. An integrated pulse profile obtained by summing all the offset observations can be seen in the bottom panel of Fig. 6. This behaviour suggests that PSR J1757−1500 is sporadically exhibiting mode changing. Profile changes are observed in pulsars in a number of ways, from short term mode changing (Backer 1970a) to long-term changes as e.g. in intermittent pulsars (Kramer et al. 2006) or even in regular pulsars (Lyne et al. 2010).
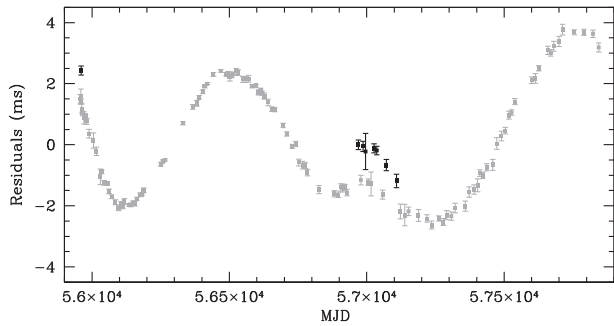
Figure 5. Timing residuals for PSR J1757−1500. The black points are those to which a phase jump needs to be applied to realign them with the rest (grey points) and summing which, the bottom profile in Fig 6 was created. The last three data points are not shown in the plot, to keep the vertical axis smaller and the phase jump visible.
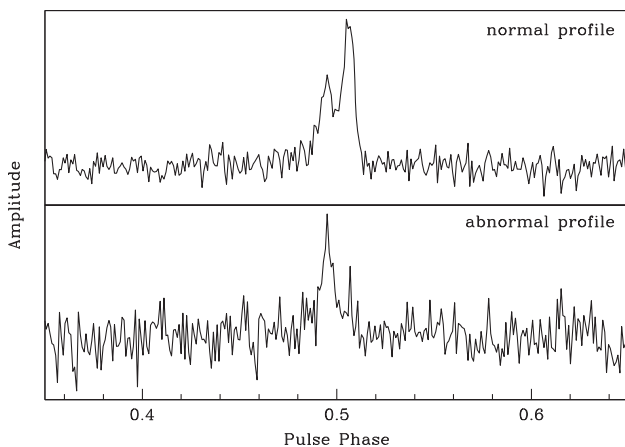

Figure 6. Comparison between the standard 'normal' pulse profile for PSR J1757−1500 (top panel) and the profile obtained summing in phase only the offset black points in Fig. 5. The profiles are zoomed in to the phase range 0.38–0.62.

Because of the low S/N of the profiles of the individual observations (on average eight, over an average integration time of 15 min), assessing more specific details for the profile changes is, unfortunately, not easily possible: we do not have enough statistics. This prevents us from obtaining information on possible changes occurring on time-scales shorter than the individual observations themselves. This, in turn, permits us to only place a lower limit on the frequency of the occurrence of the single-peaked mode, present in eight observations out of 128, all but one of which concentrated within 138 d. This apparent sporadicity is at odds with what observed in other moding pulsars, in which the profile changes occur on shorter time-scales and with a somewhat more regular cadence. These changes may be more like those seen in e.g. Dai et al. (2018) for PSR J1119−6127, or by Karastergiou et al. (2011) in PSR J0738−4042.

The small number and short duration of the observations showing offset ToAs, hence having a detectable profile variation, makes also impossible to check if mode changes are accompanied by spin-down changes, as observed e.g. for intermittent pulsars (Kramer et al. 2006; Lyne et al. 2017b) and as theorized to explain nulling and mode-changing phenomena (Timokhin 2010).
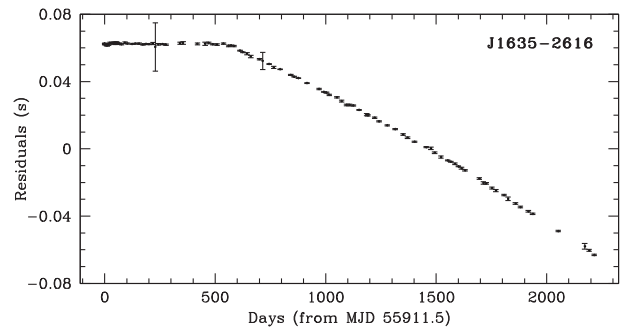

Figure 7. Timing residuals for PSR J1635−2616 relative to the timing solution before the glitch.

4.5 Pulsars with timing instabilities

4.5.1 A glitch from PSR J1635−2616

Glitches are still poorly understood instabilities in the otherwise regular spin evolution of pulsars: they manifest themselves as sudden changes of the pulsar rotation, usually followed by a slow recovery towards the pre-glitch values.

PSR J1635−2616 showed a glitch around MJD 56458(6), with a frequency variation $\delta_\nu = 1.35(5) \times 10^{-9}$ and a barely significant variation of the spin-down rate $\delta_{\dot\nu} = 5(2) \times 10^{-18}$ (the errors in parentheses are quoted at 1σ). With a characteristic age of 1.9 Myr and a single glitch in approximately 6.5 yr, the glitch rate is typical for this type of pulsar, and while it is a small glitch, it is not unusual for the observed period derivative (Espinoza et al. 2011).

Fig. 7 shows the timing residuals for PSR J1635−2616 relative to the timing solution before the glitch.

4.5.2 Timing noise

Among the pulsars that we have timed for multiple years, four (J1719−2330, J1757−1500, J1840−0445, and J1902−1036) show unmodelled long-term instabilities in their rotation (timing noise; see e.g. Hobbs, Lyne & Kramer 2006a). PSR J1902−1036 shows only a relatively small amount of timing noise so that its timing residuals are easily 'whitened' by adding to the fit the spin frequency second derivative $\ddot\nu$ only. To flatten the residuals of other three pulsars, instead, we had to fit multiple extra frequency derivatives. Fig. 8 shows the timing residuals for these three pulsars after the cubic term only ($\ddot\nu$) has been removed.

Table 7 reports the fitted value of $\ddot\nu$, the pre- and post-whitening rms of the residuals, the number of spin frequency derivatives used to flatten the timing residuals, and the values of the stability parameter $\Delta_8 = \log_{10}[t^3|\ddot\nu| \times 1/(6\nu)]$ (Arzoumanian et al. 1994), (arbitrarily) measured over data spans of 10^8 s.

Our data for the pulsars affected by timing noise cover close to twice 10^8 s; we report the average of the Δ_8 parameters obtained for the first and the last 10^8 s of data. The Δ_8 values for our three pulsars are in line with what is observed for other pulsars affected by timing noise; in particular our small sample appears to follow the relation between timing noise and spin-down rate first found by Arzoumanian et al. (1994) and refined by Hobbs, Lyne & Kramer (2010).

A magnetospheric origin for timing noise has been proposed by Lyne et al. (2010) who showed that, in several cases, the observed spin irregularity can derive from abrupt changes in the spin-down rate, typically between two values, which are sometimes linked to
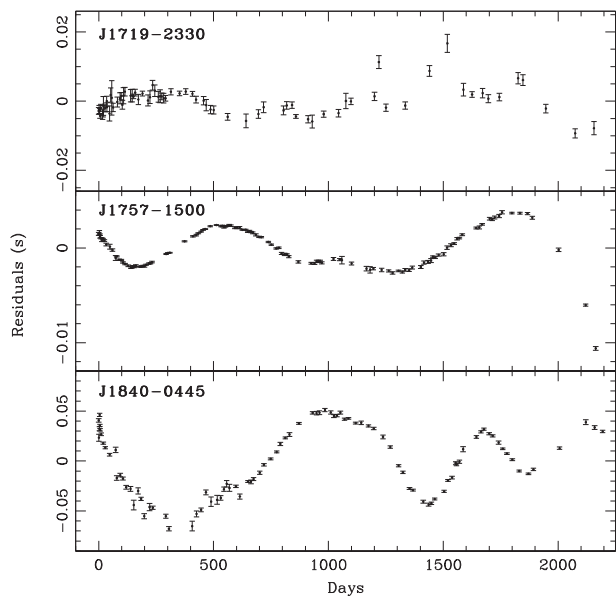
Figure 8. Timing residuals for the three noisy pulsars of our sample, after fitting for astrometric and spin parameters up to ÿ. Day 0 is the beginning of the data span as reported in Table 3, column 9.

Table 7. For each pulsar affected by timing noise, the table lists the frequency second derivative (at the epochs reported in Table 3), the rms of the timing residual obtained by fitting up to ÿ, the rms of the whitened residuals, the number of spin frequency derivatives fitted for to whiten the timing residuals, and the average stability parameter. Number in parentheses are TEMPO2 2σ errors on the last quoted digit(s). Note that, over 10^8 s, PSR J1902−1036 does not show timing noise, hence no Δ_8 is reported.

PSR	$\ddot{\nu}$ $(10^{-25}$ s$^{-3})$	rms$_{pre}$ (ms)	rms$_{post}$ (ms)	#ν	Δ_8
J1719−2330	−4.3(10)	3.15	1.27	4	−1.41
J1757−1500	−7.2(12)	1.82	0.13	11	−1.28
J1840−0445	−137(7)	28.31	3.08	12	−0.9
J1902−1036	−0.54(11)	0.99	–	2	–

pulse shape changes. A future study, using longer data spans, will investigate if this is the case also for these noisy HTRU-med pulsars.

5 COMPARISON BETWEEN HTRU-MED AND OTHER SURVEYS

The High Time Resolution Unverse Survey has been one of the most successful pulsar search experiments of the recent years, especially in terms of MSP discoveries. Its intermediate-latitude section, covering the Galactic latitude range −15° to +15°, in particular, has discovered 113 new pulsars to date, 29 of which are (fully and mildly) recycled pulsars.

Based on the ATNF pulsar catalogue, 1135 Galactic radio pulsars were already known in the survey area, 42 of which were recycled objects. The ratio of recycled over ordinary PSRs in HTRU-med is more than seven times higher than that of the previously known sample. Even the ratio for the previous Parkes experiment covering roughly the same area, the SWIN$_{MED}$ (Edwards et al. 2001), mainly aimed at finding MSPs, was three times smaller than that of HTRU-med.

This confirms that our survey digital signal processor (BPSR), with a 8× better frequency resolution and a >2× better timing
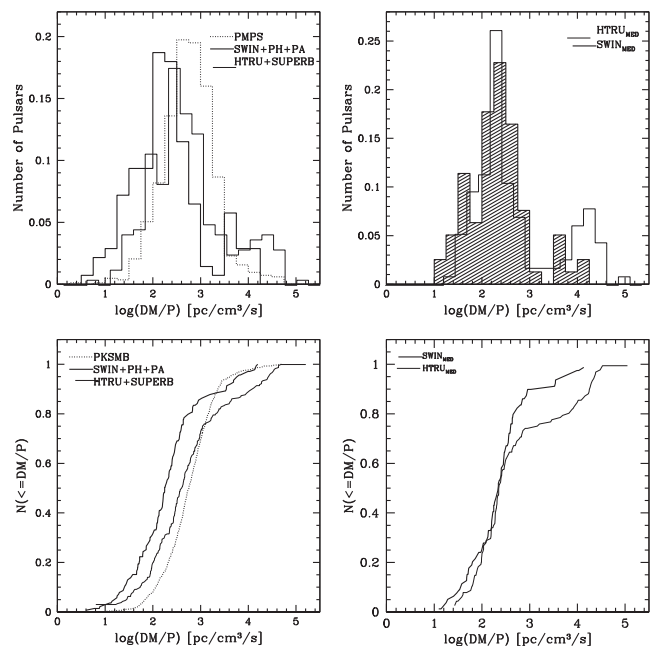

Figure 9. Normalized histograms (top) and cumulative distributions (bottom) of DM/P for Parkes survey discoveries. Left: the dotted curve is for the Galactic plane multibeam survey PMPS (Manchester et al. 2001), with a 3-MHz frequency resolution and a 250 μs time resolution; the solid thin curve is for surveys with the same frequency resolution, but 2× finer time resolution (SWIN, Edwards et al. 2001; Jacoby et al. 2009; PH, Burgay et al. 2006; and PA, Burgay et al. 2013); the solid thick curve is for the most recent surveys using the BPSR digital backend, with 0.39-MHz frequency resolution and 64 μs time resolution (HTRU, Keith et al. 2010 and SUPERB, Keane et al. 2018). Right: comparison of intermediate-latitude Parkes surveys only. The shaded histogram is for the SWIN$_{MED}$ surveys, the thick solid line for HTRU-med.

resolution than the major previous Parkes pulsar surveys, was very well suited to find the rarer, faster MSPs, which often prove to be interesting and extreme objects. The only other pulsar survey, although covering a different area of the sky, that can compare to HTRU-med in terms of MSP discovery rate, is the Arecibo PALFA survey (Cordes et al. 2006), with 17 per cent of recycled pulsars in 188 discoveries[9]. This similarity is not surprising, since PALFA works at the same frequency and has almost equal timing and spectral resolution to HTRU-med.

Another interesting number to consider, is the dispersion measure over spin period ratio DM/P, a parameter that can be used to estimate the depth of an MSP search. DM/P of HTRU-med recycled pulsars, is, on average, greater than that of previous experiments covering the same regions of the sky, confirming the effectiveness of our observing strategy. The mean value of DM/P for HTRU-med discoveries is, indeed, 90 per cent larger than that of the previously known recycled pulsars in the area, and the median value is 120 per cent larger.

Fig. 9 shows, on the left, a comparison of the DM/P histograms for Parkes surveys of increasing time and frequency resolution: from the Galactic plane multibeam survey (PMPS; Manchester et al. 2001), that used an analogue filterbank with 3-MHz channels and a sampling time of 250 μs, to the high and intermediate-latitude surveys (PH and SWIN; Edwards et al. 2001; Burgay et al. 2006;

[9]http://www.naic.edu/palfa/newpulsars/

Jacoby et al. 2009), that, together with PMPS extension on the Perseus Arm (PA; Burgay et al. 2013), used the same backend, but a 125 μ sampling time, to the HTRU and SUPERB (Keane et al. 2018) surveys, using the BPSR digital backend with 0.39-MHz channels and a 64 μs sampling time. While PMPS, covering the denser plane of the Galaxy, has a larger fraction of non-recycled, high DM pulsars, the highest DM/P objects, with small spin periods and large DMs, increase with the finer time and frequency resolution of subsequent experiments. The improvement (especially for recycled pulsar) is clearer and unbiased if we compare (Fig. 9, right) the intermediate-latitude part of HTRU only, with SWIN$_{MED}$, covering the same area in the sky (hence regions with the same free electron content). We note that we chose to show only discoveries, and not also redetections, because the latter can be biased by the prior knowledge of the existence of a pulsar with a specific P and DM: even with a low S/N and a broadened profile, a previously known pulsar can be safely recognized and listed as redetection, while, if it were a new source, it might not even be considered as a candidate worth of reobservation.

The HTRU-med MSP J1804−2858, with a P of 1.49 ms and a DM of 232 pc cm^{-3} (Morello et al. 2019), is the second fastest pulsar discovered in the Galactic field, and has the second highest DM/P value of all known pulsars (the record being held by the Globular Cluster MSP J1748−2446ad; Hessels et al. 2006). In PMPS the pulse of such an extreme object would have been completely washed away, the DM-smearing being larger than the spin period, in a 3-MHz channel. Future surveys, such as the upcoming experiments with the Square Kilometre Array precursor MeerKAT (Jonas 2009), will be sensitive to even faster and/or further away objects: a pulsar with the same DM smearing that J1804−2858 has in HTRU, for instance, can be found, with MeerKAT, at DMs 50 per cent larger (hence, roughly, 50 per cent more distant, in a similarly dense environment); on the other hand, a pulsar with the same DM as J1804−2858 will have the same observed duty cycle as the one J1804−2858 has in HTRU, even with a 50 per cent shorter spin period, thanks to the improved frequency resolution of MeerKAT surveys, which will use 4096 channels over a 856 MHz bandwidth.

6 CONCLUSIONS

In this paper we have presented the discovery and timing of six more pulsars found in the intermediate-latitude part of the High Time Resolution Universe Survey, and a coherent timing solution for a further 19 HTRU-med pulsars. With these discoveries, the last coming from our standard data analysis pipeline, the total yield for HTRU-med is now 113 new pulsars, 29 of which – a record 25 per cent of the total – are recycled objects. HTRU-med has hence proven to be very effective at finding new MSPs and in particular, thanks to its time and frequency resolution, in finding objects covering previously poorly populated parameter spaces (e.g. high DMs and low P).

Among HTRU-med discoveries we can list many notable pulsars: from the binary MSP J1801+3212 (Ng et al. 2014), potentially useful to test the Strong Equivalence Principle, to the 'diamond planet' pulsar J1719−1438 (Bailes et al. 2011), shedding light on the formation mechanism of ultracompact systems. The long-period, mildly eccentric binary pulsar J1837−0822 (this work) is now the third of a small class of peculiar objects whose companion has likely lost mass without spinning the NS up. Its discovery adds a piece to the puzzle of the evolution of these systems. Also interesting for the study of binary evolution are the eclipsing Redbacks and Black Widow pulsars – one of each was found in HTRU-med (Bates

et al. 2011, 2015). Their final fate is believed to lead to the formation of isolated MSPs. Two fully recycled such objects were found in the survey area (this work and Burgay et al. 2013). Analysing eclipsing 'spider' pulsar characteristics and comparing them with those of fully recycled isolated MSPs, we found contrasting pieces of evidence: on one hand, we showed that the spin period of isolated MSPs is significantly longer than that of spiders. This, simply taking into account the dipolar spin-down, would corroborate the idea that isolated MSPs may represent a later evolutionary stage of the faster spinning eclipsing binaries. On the other hand, however, isolated pulsars are found, on average, further away from the Galactic plane than Redbacks and Black Widows. If the two shared a common evolutionary path, they should have received a similar natal kick, which would be reflected in a similar spatial distribution.

The positive outcome of HTRU-med, finally, is further highlighted by the fact that six of our MSPs have been already included in Pulsar Timing Array projects, which was one of the main goals of the intermediate part of our experiment (Keith et al. 2010).

The next step forward to find more distant, fainter, higher DM recycled pulsars will be achieved by the new surveys planned with the South African SKA precursor MeerKAT. Thanks to its superb sensitivity, its larger bandwidth and the possibility for finer time and frequency resolution, MeerKAT has the potential to discover many new peculiar and extreme objects (Stappers & Kramer 2016).

REFERENCES

Alpar M. A., Cheng A. F., Ruderman M. A., Shaham J., 1982, Nature, 300, 728
Antoniadis J. et al., 2013, Science, 340, 448
Arzoumanian Z., Nice D. J., Taylor J. H., Thorsett S. E., 1994, ApJ, 422, 671
Backer D. C., 1970a, Nature, 228, 1297
Backer D. C., 1970b, Nature, 228, 42
Bailes M. et al., 2011, Science, 333, 1717
Bailyn C. D., Grindlay J. E., 1990, ApJ, 353, 159
Barr E. D. et al., 2013, MNRAS, 435, 2234
Bassa C. G. et al., 2016, MNRAS, 456, 2196
Bates S. D. et al., 2011, MNRAS, 416, 2455
Bates S. D. et al., 2012, MNRAS, 427, 1052
Bates S. D. et al., 2015, MNRAS, 446, 4019
Bhattacharya D., van den Heuvel E. P. J., 1991, Phys. Rep., 203, 1
Blandford R., Teukolsky S. A., 1976, ApJ, 205, 580
Burgay M. et al., 2006, MNRAS, 368, 283
Burgay M. et al., 2013, MNRAS, 429, 579
Burgay M. et al., 2013, MNRAS, 433, 259
Camilo F., Ransom S. M., Chatterjee S., Johnston S., Demorest P., 2012, ApJ, 746, 63
Chen H.-L., Chen X., Tauris T. M., Han Z., 2013, ApJ, 775, 27
Cordes J. M., Lazio T. J. W., 2002, preprint (astro-ph/020715)

Cordes J. M. et al., 2006, ApJ, 637, 446

Dai S. et al., 2018, MNRAS, 480, 3584

Edwards R. T., Bailes M., van Straten W., Britton M. C., 2001, MNRAS, 326, 358

Espinoza C. M., Lyne A. G., Stappers B. W., Kramer M., 2011, MNRAS, 414, 1679

Folkner W. M., Williams J. G., Boggs D. H., 2009, in Pollara F., ed. IPN Progress Report 42-178, 'The Planetary and Lunar Ephemeris DE 412'. NASA Jet Propulsion Laboratory, California Institute of Technology, Pasadeena, California

Gajjar V., Yuan J. P., Yuen R., Wen Z. G., Liu Z., Wang N., 2017, 863, 2

Hessels J. W. T., Ransom S. M., Stairs I. H., Freire P. C. C., Kaspi V. M., Camilo F., 2006, Science, 311, 1901

Hobbs G., Lyne A., Kramer M., 2006a, Chin. J. Astron. Astrophys., 6, 169

Hobbs G., Lyne A. G., Kramer M., 2010, MNRAS, 402, 1027

Hobbs G. B., Edwards R. T., Manchester R. N., 2006b, MNRAS, 369, 655

Hotan A. W., van Straten W., Manchester R. N., 2004, Publ. Astron. Soc. Aust., 21, 302

Jacoby B. A., Bailes M., Ord S., Knight H., Hotan A., Edwards R. T., Kulkarni S. R., 2009, ApJ, 699, 2009

Jonas J., 2009, The MeerKAT SKA precursor telescope. in Heald G., Serra P., eds, Panoramic Radio Astronomy: Wide-field 1-2 GHz Research on Galaxy Evolution. Proceedings of Science, Trieste, p. 4

Karastergiou A., Roberts S. J., Johnston S., Lee H., Weltevrede P., Kramer M., 2011, MNRAS, 415, 251

Keane E. F. et al., 2018, MNRAS, 473, 116

Keith M. J. et al., 2010, MNRAS, 409, 619

Knispel B. et al., 2013, ApJ, 774, 93

Kramer M., Lyne A. G., O'Brien J. T., Jordan C. A., Lorimer D. R., 2006, Science, 312, 549

Kulkarni S. R., Narayan R., 1988, ApJ, 335, 755

Lorimer D. R., Bailes M., McLaughlin M. A., Narkevic D. J., Crawford F., 2007, Science, 318, 777

Lorimer D. R., Kramer M., 2005, Handbook of Pulsar Astronomy. Cambridge Univ. Press, Cambridge

Lorimer D. R., Lyne A. G., McLaughlin M. A., Kramer M., Pavlov G. G., Chang C., 2012, ApJ, 758, 141

Lorimer D. R. et al., 2006, MNRAS, 372, 777

Lyne A., Hobbs G., Kramer M., Stairs I., Stappers B., 2010, Science, 329, 408

Lyne A. G., Smith F. G., 1990, Pulsar Astronomy. Cambridge Univ. Press, Cambridge

Lyne A. G., Stappers B. W., Keith M. J., Ray P. S., Kerr M., Camilo F., Johnson T. J., 2015, MNRAS, 451, 581

Lyne A. G. et al., 2017a, ApJ, 834, 137

Lyne A. G. et al., 2017b, ApJ, 834, 72

Manchester R. N., Hobbs G. B., Teoh A., Hobbs M., 2005, AJ, 129, 1993

Manchester R. N. et al., 1996, MNRAS, 279, 1235

Manchester R. N. et al., 2001, MNRAS, 328, 17

Michel F. C., 1982, Rev. Mod. Phys., 54, 1

Morello V. et al., 2019, MNRAS, 483, 3673

Ng C. et al., 2014, MNRAS, 439, 1865

Ng C. et al., 2015, MNRAS, 450, 2922

Phinney E. S., 1992, Phil. Trans. R. Soc., 341, 39

Phinney E. S., Kulkarni S. R., 1994, ARA&A, 32, 591

Roberts M. S. E., 2013, in van Leeuwen J., ed., Proc. IAU Symp. Vol. 291, Neutron Stars and Pulsars: Challenges and Opportunities after 80 years, Kluwer, Dordrecht, p. 127

Ruderman M., Shaham J., Tavani M., 1989, ApJ, 336, 507

Stappers B., Kramer M., 2016, in Taylor R., Camilo F., Leeuw L., Moodley K., eds, Proceedings of MeerKAT Science: On the Pathway to the SKA. 25-27 May, 2016 Stellenbosch, South Africa (MeerKAT2016), Proceedings of Science, Trieste, p. 9

Stappers B. W. et al., 1996, ApJ, 465, L119

Staveley-Smith L. et al., 1996, Publ. Astron. Soc. Aust., 13, 243

Surnis M. P., Joshi B. C., McLaughlin M. A., Gajjar V., 2013, in van Leeuwen J., ed., Proc. IAU Symp., Vol. 291. Neutron Stars and Pulsars: Challenges and Opportunities after 80 years. Kluwer, Dordrecht, p. 508

Tauris T. M., Bailes M., 1996, A&A, 315, 432

Tauris T. M., Langer N., Kramer M., 2012, MNRAS, 425, 1601

Tauris T. M., Sennels T., 2000, A&A, 355, 236

Thornton D. et al., 2013, Science, 341, 53

Timokhin A. N., 2010, MNRAS, 408, L41

van den Heuvel E. P. J., van Paradijs J., 1988, Nature, 334, 227

Verbunt F., van den Heuvel E. P. J., van Paradijs J., Rappaport S. A., 1987, Nature, 329, 312

Wang N., Manchester R. N., Johnston S., 2007, MNRAS, 377, 1383

Yao J. M., Manchester R. N., Wang N., 2017, ApJ, 835, 29

SUPPORTING INFORMATION

Supplementary data are available at *MNRAS* online.

HTRUmedlat.gl.gb

Please note: Oxford University Press is not responsible for the content or functionality of any supporting materials supplied by the authors. Any queries (other than missing material) should be directed to the corresponding author for the article.

[1] *INAF - Osservatorio Astronomico di Cagliari, via della Scienza 5, I-09047 Selargius (CA), Italy*

[2] *Jodrell Bank Centre for Astrophysics, University of Manchester, Alan Turing Building, Oxford Road, Manchester M13 9PL, UK*

[3] *Centre for Astrophysics and Supercomputing, Swinburne University of Technology, Mail H39, PO Box 218, VIC 3122, Australia*

[4] *ARC Centre of Excellence for Gravitational Wave Discovery (OzGrav), Swinburne University of Technology, Mail H11, PO Box 218, VIC 3122, Australia*

[5] *Max-Planck-Institut für Radioastronomie, Auf dem Hügel 69, D-53121 Bonn, Germany*

[6] *International Centre for Radio Astronomy Research, Curtin University, Bentley, WA 6102, Australia*

[7] *Center for Gravitational Waves and Cosmology, West Virginia University, Chestnut Ridge Research Building, Morgantown, WV 26505, USA*

[8] *CSIRO Astronomy & Space Science, Australia Telescope National Facility, PO Box 76, Epping, NSW 1710, Australia*

[9] *SKA Organisation, Jodrell Bank Observatory, Macclesfield, SK11 9DL, UK*

[10] *Department of Physics and Astronomy, University of British Columbia, 6224 Agricultural Road, Vancouver, BC V6T 1Z1, Canada*

[11] *ASTRON, the Netherlands Institute for Radio Astronomy, Postbus 2, NL-7990 AA Dwingeloo, the Netherlands*

[12] *Institute for Radio Astronomy & Space Research, Auckland University of Technology, Private Bag 92006, Auckland 1142, New Zealand*

[13] *Fakultät fur Physik, Universität Bielefeld, Postfach 100131, D-33501 Bielefeld, Germany*

[14] *LPC2E - Université d'Orléans / CNRS, F-45071 Orléans CEDEX 2, France*

This paper has been typeset from a TEX/LATEX file prepared by the author.